Observation of anticorrelation in incoherent thermal light fields

Hui Chen, Tao Peng, Sanjit Karmakar, Zhenda Xie, and Yanhua Shih
Department of Physics, University of Maryland, Baltimore County, Baltimore, Maryland 21250, USA
(Received 18 August 2010; published 19 September 2011)

We wish to report a recent experimental observation of anticorrelation from first-order and second-order incoherent thermal fields in the joint photodetection of two independent photodetectors. In the view of classical theory, the nontrivial second-order correlation of thermal light is caused by the statistical correlation of intensity fluctuations, which can be observed only from first-order coherent thermal radiations. What is the physical cause of this observed anticorrelation, then?

DOI: 10.1103/PhysRevA.84.033835 PACS number(s): 42.50.Ar, 42.50.Ct, 42.50.Dv

I. INTRODUCTION

In 1956, Hanbury Brown and Twiss (HBT) discovered a nontrivial temporal intensity correlation

$$\Gamma^{(2)}(\tau_A,\tau_B) = \langle I(\tau_A)\rangle\langle I(\tau_B)\rangle[1+|\gamma^{(1)}(\tau_A,\tau_B)|^2] \sim I_0^2\left\{1+\mathrm{sinc}^2\left[\frac{\Delta\omega(\tau_A-\tau_B)}{2}\right]\right\} \quad (1)$$

and a nontrivial spatial intensity correlation

$$\Gamma^{(2)}(\vec{\rho}_A,\vec{\rho}_B) = \langle I(\tau_A)\rangle\langle I(\tau_B)\rangle[1+|\gamma^{(1)}(\vec{\rho}_A,\vec{\rho}_B)|^2] \sim I_0^2\left\{1+\mathcal{S}^2\left[\frac{\pi\Delta\theta|\vec{\rho}_A-\vec{\rho}_B|}{\lambda}\right]\right\} \quad (2)$$

in the joint measurement of thermal radiation [1,2]. Figure 1 shows a fiber-based modern HBT interferometer which can measure both temporal and spatial intensity correlations. In Eqs. (1) and (2),

$$\Gamma^{(2)}(\tau_A,\tau_B) = \langle I(\tau_A)I(\tau_B)\rangle,$$
$$\Gamma^{(2)}(\vec{\rho}_A,\vec{\rho}_B) = \langle I(\vec{\rho}_A)I(\vec{\rho}_B)\rangle$$

are the temporal and spatial intensity correlation, respectively. $\gamma^{(1)}(\tau_A,\tau_B)$ and $\gamma^{(1)}(\vec{\rho}_A,\vec{\rho}_B)$ are the degree of first-order temporal and spatial coherence of the thermal radiation, respectively. The sinc function and the sombrero-like function $\mathcal{S}$ are defined as

$$\mathrm{sinc}(x) = \frac{\sin(x)}{x} \quad \text{and} \quad \mathcal{S}(x) = \frac{2J_1(x)}{x},$$

where $J_1(x)$ is the first-order Bessel function, $\tau_A = t_A - z_A/c$ and $\tau_B = t_B - z_B/c$ are the temporal coordinates of the two photodetection events (t_j and z_j with $j = A,B$ are the registration times and longitudinal coordinates of the photodetection event), $\Delta\omega$ is the spectral bandwidth of the thermal radiation, $\vec{\rho}_A$ and $\vec{\rho}_B$ are the transverse coordinates of the two photodetectors D_A and D_B, $\Delta\theta$ is the angular size of the far-field thermal source, and λ is the wavelength of the radiation.

It is easy to see from Eqs. (1) and (2), in a temporal HBT interferometer, that the temporally randomly distributed thermal light has a twice greater chance of triggering a joint detection within its coherence time, $\tau_c = 2\pi/\Delta\omega$. In a spatial HBT interferometer, the spatially randomly distributed thermal light exhibits a twice greater chance of joint detection within a coherent length, $l_c = \lambda/\Delta\theta$. This property has been widely utilized in space and astrophysics applications.

It was recently found that for a large angular sized thermal source the spatial correlation is effectively within a physical "point," indicating a typical nonlocal position-position correlation of a measured photon pair [3]. In the language of Einstein, Podolsky, and Rosen (EPR) [4], in a joint detection of two photons, neither photon one nor photon two knows precisely where to go when they are created at the thermal source; however, if one of them is observed at a certain space-time point the other one must have two times the probability to be found at the same space-time point. The point-to-point correlation of thermal light has been utilized for reproducing ghost images in a lensless configuration [5].

In classical theory, thermal light belongs to Gaussian light in terms of its statistical behavior. Thermal light is produced from a stochastic process. In a thermal source, such as a thermal star, the radiations created from a large number of atomic transitions are all independent. Each atomic transition creates its photon independently and randomly.

Figure 2 schematically illustrates the propagation of thermal radiation.[1] To simplify the picture we assume a one-dimensional source with a large number of independent point subsources randomly ranging from $-D/2$ to $D/2$. Each point subsource, such as the jth or the kth atomic transition, randomly radiates independent spherical waves to the 4π solid angle. Assuming the jth or the kth subsource each created a photon at time t_0, after a one-year propagation, each spherical wave front would develop a radius of one light-year. In the view of quantum mechanics, each photon has an equal chance to be detected by a pointlike photon counting detector at any point on the one-light-year sphere, although the theory cannot predict its precise position. Einstein questioned the physics behind such an observation in the early days of quantum mechanics and asked a simple question: How much time does it takes for the one-light-year wave sphere to collapse into one photodetection event? Today, although we still ask the same question, we are not surprised to observe a photodetection event of a single photon from a light-year distant star in our everyday life. Since 1956, we have been facing a picture that is

[1]One should not confuse the propagation of thermal light with the propagation of a laser beam. A laser beam propagates coherently. After propagating a distance, a large transverse sized laser beam may keep a slightly enlarged beam size due to diffraction. Thermal light propagates incoherently which is very different from a laser beam.

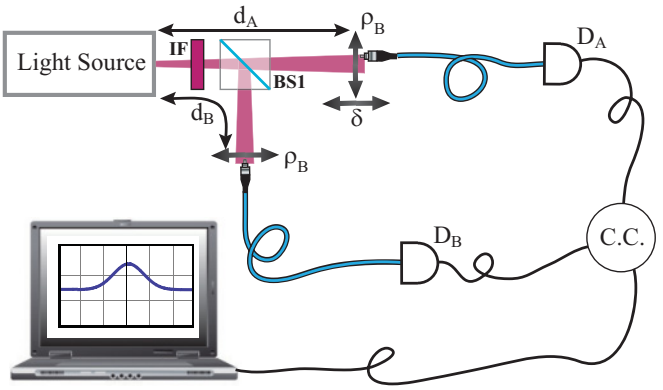

FIG. 1. (Color online) Schematic of a modern HBT interferometer which measures both temporal and spatial correlation of thermal light by scanning the optical fiber tips longitudinally or transversely. The two optical fibers are coupled into photon counting detectors, D_A and D_B, and a coincidence counter (C.C.) is employed for HBT correlation measurement. The spectral bandwidth of the radiation, $\Delta\omega$, is determined by IF (an interference filter). The opening angle of the thermal source is $\Delta\theta$.

a bit more complicated than Einstein's: In Fig. 2, neither the jth photon nor the kth photon knows precisely where to go when they are created in the source, and each will repeat the story of Einstein and appear randomly at any point on their light-year spherical wave front after a light-year propagation. However, if one of them is observed at an arbitrary point on the sphere, the other one must have two times the chance of being observed at the same point. There is no doubt that the experimental observations have confirmed the *physical truth* of the effect. Naturally, we ask ourselves another simple question: What is the *physical cause* that forces a twice greater probability for the two independent light-year wave spheres to collapse into one joint-detection event at $\tau_A = \tau_B$ and $\vec{\rho}_A = \vec{\rho}_B$? Unlike the entangled photon pair, the jointly measured photons from a thermal source are just two independent photons that fall into the coincidence time window by chance only.

It seems that the problems come from the concept of photons or the quantum picture of light, as Hanbury Brown pointed out in his book [1]. It would be very important to find

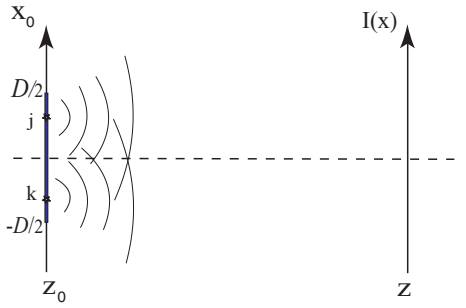

FIG. 2. (Color online) A large number of independent point subsources, such as the jth and kth, are randomly distributed on the plane of a thermal source. These point subsources randomly radiate independent spherical waves. Due to the stochastic character of the source, these independent subintensities are simply added together and yield a constant intensity distribution on any transverse planes.

out the truth: What is the reason for the concept of a photon to face difficulties in front of HBT? Nevertheless, historically the HBT phenomenon was interpreted as the statistical correlation of *intensity fluctuations* [6].

In the classical theory of light, the joint detection between two individual pointlike photodetectors, D_A and D_B, measures the statistical correlation of intensities at space-time coordinates $(\mathbf{r}_A,t_A)$ and $(\mathbf{r}_B,t_B)$:

$$\begin{aligned}\Gamma^{(2)}(\mathbf{r}_A,t_A;\mathbf{r}_B,t_B) &= \langle E^*(\mathbf{r}_A,t_A)E(\mathbf{r}_A,t_A)E^*(\mathbf{r}_B,t_B)E(\mathbf{r}_B,t_B)\rangle \\ &= \Gamma^{(1)}_{AA}\Gamma^{(1)}_{BB} + \Gamma^{(1)}_{AB}\Gamma^{(1)}_{BA}, \end{aligned} \tag{3}$$

where

$$\begin{aligned}\Gamma^{(1)}_{AA} &= \langle E^*(\mathbf{r}_A,t_A)E(\mathbf{r}_A,t_A)\rangle, \\ \Gamma^{(1)}_{BB} &= \langle E^*(\mathbf{r}_B,t_B)E(\mathbf{r}_B,t_B)\rangle, \\ \Gamma^{(1)}_{AB} &= \Gamma^{*(1)}_{BA} = \langle E^*(\mathbf{r}_A,t_A)E(\mathbf{r}_B,t_B)\rangle.\end{aligned}$$

Here $\Gamma^{(1)}_{AA}$ and $\Gamma^{(1)}_{BB}$ are known as self-coherence functions, and $\Gamma^{(1)}_{AB}$ and $\Gamma^{(1)}_{BA}$ are the mutual coherence functions.

In Eq. (3), we have applied the standard Gaussian statistics of thermal light [7,8]:[2]

$$\begin{aligned}\langle X_1\,X_2\,X_3\,X_4\rangle &= \langle X_1X_2\rangle\langle X_3X_4\rangle + \langle X_1X_3\rangle\langle X_2X_4\rangle \\ &\quad + \langle X_1X_4\rangle\langle X_2X_3\rangle.\end{aligned}$$

Comparing with

$$\begin{aligned}\Gamma^{(2)}(\mathbf{r}_A,t_A;\mathbf{r}_B,t_B) &= \langle I(\mathbf{r}_A,t_A)I(\mathbf{r}_B,t_B)\rangle \\ &= \langle I(\mathbf{r}_A,t_A)\rangle\langle I(\mathbf{r}_B,t_B)\rangle \\ &\quad + \langle \Delta I(\mathbf{r}_A,t_A)\Delta I(\mathbf{r}_B,t_B)\rangle, \end{aligned} \tag{4}$$

the nontrivial HBT correlation comes from the second term of Eq. (4), which is considered the statistical correlation of *intensity fluctuations* $\langle \Delta I(\mathbf{r}_A,t_A)\Delta I(\mathbf{r}_B,t_B)\rangle$.

To support their intensity fluctuation interpretation, HBT provided a reasonable physical picture based on the far-field measurement of distant stars: In the far-field plane, when two detectors are placed closed enough, they measure the same optical mode and thus experience the same intensity fluctuations; however, while they are moved apart from each other, the two detectors start to measure different modes and experience random intensity fluctuations.

Quantum mechanics provides a different point of view. A joint-photodetection event between D_A and D_B measures the probability of observing two photons jointly at space-time coordinates $(\mathbf{r}_A,t_A)$ and $(\mathbf{r}_B,t_B)$, which is proportional to the second-order coherence function of the radiation $G^{(2)}(\mathbf{r}_A,t_A;\mathbf{r}_B,t_B)$. If there exist two alternative ways for a pair of photons, either entangled photons or randomly paired photons that fall into the coincidence time window by chance, to produce a joint-photodetection event, the two probability

[2]In the theory of classical statistics, a standard approach to calculate an ensemble average that involves four fields is applying Gaussian statistics to break it into a sum of ensemble averages each involving two fields only.

amplitudes must be linearly superposed in the probability calculation by using Glauber-Scully theory [9,10]:

$$
\begin{aligned}
&G^{(2)}(\mathbf{r}_A,t_A;\mathbf{r}_B,t_B)\\
&\quad=\langle\langle\hat{E}^{(-)}(\mathbf{r}_A,t_A)\hat{E}^{(-)}(\mathbf{r}_B,t_B)\hat{E}^{(+)}(\mathbf{r}_B,t_B)\hat{E}^{(+)}(\mathbf{r}_A,t_A)\rangle_{\mathrm{QM}}\rangle_{\mathrm{Es}}\\
&\quad\simeq\left\langle\sum_j P_j|\Psi_j(\mathbf{r}_A,t_A;\mathbf{r}_B,t_B)|^2\right\rangle_{\mathrm{Es}}\\
&\quad=\left\langle\sum_{m,n} P_{mn}|\mathscr{A}_{mn}(\mathbf{r}_A,t_A;\mathbf{r}_B,t_B)+\mathscr{A}_{nm}(\mathbf{r}_A,t_A;\mathbf{r}_B,t_B)|^2\right\rangle_{\mathrm{Es}}\\
&\quad\propto\left\langle\sum_{m,n} P_{mn}|\mathscr{A}_{mn}(\mathbf{r}_A,t_A;\mathbf{r}_B,t_B)|^2\right\rangle_{\mathrm{Es}}\\
&\qquad+\left\langle\sum_{m,n} P_{mn}\mathscr{A}_{mn}(\mathbf{r}_A,t_A;\mathbf{r}_B,t_B)\mathscr{A}^*_{nm}(\mathbf{r}_A,t_A;\mathbf{r}_B,t_B)\right\rangle_{\mathrm{Es}},
\end{aligned}
\tag{5}
$$

where

$$\Psi_j(\mathbf{r}_A,t_A;r_B,t_B)=\langle 0|\hat{E}^{(+)}(\mathbf{r}_B,t_B)\hat{E}^{(+)}(\mathbf{r}_A,t_A)|\psi_j\rangle.$$

In Eq. (5), the subscript "Es" denotes an ensemble average; P_{mn} stands for the probability for the m-nth photons to create a joint-photodetection event; $\hat{E}^{(+)}(\mathbf{r}_B,t_B)$ and $\hat{E}^{(+)}(\mathbf{r}_A,t_A)$ are the field operators at space-time coordinates $(\mathbf{r}_B,t_B)$ and $(\mathbf{r}_A,t_A)$. $|\psi_j\rangle$ is the state of the jth paired photons. $\Psi_j(\mathbf{r}_A,t_A;\mathbf{r}_B,t_B)$ is defined as the effective two-photon wave function for the jth measured photon pair which produced the jth joint-photodetection event.

$$
\begin{aligned}
\mathscr{A}_{mn}(\mathbf{r}_A,t_A;\mathbf{r}_B,t_B)&=\langle 0|E^{(+)}(\mathbf{r}_B,t_B)E^{(+)}(\mathbf{r}_A,t_A)|\psi_{mn}\rangle,\\
\mathscr{A}_{nm}(\mathbf{r}_A,t_A;\mathbf{r}_B,t_B)&=\langle 0|E^{(+)}(\mathbf{r}_B,t_B)E^{(+)}(\mathbf{r}_A,t_A)|\psi_{nm}\rangle
\end{aligned}
$$

are the superposed two-photon amplitudes corresponding to two different yet indistinguishable alternatives that the jth paired photons m and n are detected at $(\mathbf{r}_A,t_A)$ and $(\mathbf{r}_B,t_B)$, respectively, or detected at $(\mathbf{r}_B,t_B)$ and $(\mathbf{r}_A,t_A)$, respectively.

In the view of quantum theory of light, the HBT correlation of temporal and spatial "peaks" observed from Fig. 1 is caused by an interference which involves the superposition of two different yet indistinguishable two-photon probability amplitudes of $\mathscr{A}_{mn}(\mathbf{r}_A,t_A;\mathbf{r}_B,t_B)$ and $\mathscr{A}_{nm}(\mathbf{r}_A,t_A;\mathbf{r}_B,t_B)$. When the two amplitudes are quantum mechanically indistinguishable, or overlapped in space-time, the cross term $\langle\sum_{m,n} P_{mn}\mathscr{A}_{mn}(\mathbf{r}_A,t_A;\mathbf{r}_B,t_B)\mathscr{A}^*_{nm}(\mathbf{r}_A,t_A;\mathbf{r}_B,t_B)\rangle_{\mathrm{Es}}$ contributes a nonzero value to the joint measurement of D_A and D_B, resulting in a "peak" to the correlation. However, if the two photodetectors are moved far apart causing $\mathscr{A}_{mn}(\mathbf{r}_A,t_A;\mathbf{r}_B,t_B)$ and $\mathscr{A}_{nm}(\mathbf{r}_A,t_A;\mathbf{r}_B,t_B)$ to not overlap, the cross term $\langle\sum_{m,n} P_{mn}\mathscr{A}_{mn}(\mathbf{r}_A,t_A;\mathbf{r}_B,t_B)\mathscr{A}^*_{nm}(\mathbf{r}_A,t_A;\mathbf{r}_B,t_B)\rangle_{\mathrm{Es}}$ becomes zero. The correlation turns into a trivial constant. Furthermore, the quantum interference picture does not require a far-field measurement. It works in both the Fraunhofer far field and Fresnel near field.

It is important to notice that the cross terms of two probability amplitudes may be nonzero in certain experimental conditions, such as that of the reported measurement, even when there are no synchronous intensity fluctuations between the A and B fields. For instance, $\Gamma^{(1)}_{AB}=0$ as long as the A and B fields are mutually incoherent. However, when $\Gamma^{(1)}_{AB}=0$, intensity fluctuation theory only predicts a nontrivial correlation as we can see in Eq. (3).

Therefore, it is natural to ask: Can we design an experiment to distinguish the statistical theory of intensity fluctuation correlation from the quantum theory of two-photon interference? We have found a positive answer: If we can find two intensities I_A and I_B with $\langle\Delta I_A\Delta I_B\rangle=0$, i.e., we are sure that the two intensities have no intensity fluctuation correlation at all, or say the radiations of A and B are first-order and second-order incoherent, can we still observe any nontrivial correlation from the two? This question can be easily answered experimentally. First, it is not too difficult to produce two first-order and second-order incoherent fields A and B. In an HBT setup, either in the far field or in the near field, if we move the slits A and B outside the coherent area to force $\Gamma^{(1)}_{AB}=\langle E^*_A E_B\rangle=0$ and $\Gamma^{(2)}_{AB}=\langle E^*_A E_A E^*_B E_B\rangle=$ constant, we are sure the intensity fluctuations of the A field and B field have no correlation [11]. Second, it is not too difficult to bring the incoherent radiations A and B together by a beam splitter and to measure the second-order correlation again. If we observe a constant correlation, the intensity fluctuation correlation picture world be correct, because whatever a beam splitter does, $\langle\Delta I(\mathbf{r}_A,t_A)\Delta I(\mathbf{r}_B,t_B)\rangle=0$ cannot be changed. However, if we observe a nontrivial correlation from the joint measurement of two photodetectors, and we can identify the contributions from the self-correlations of the radiation A and the radiation B, respectively, and exclude the self-correlations from the measurement, i.e., we are sure the nontrivial correlation is the correlation between radiations A and B only, it would be natural to put a question mark to the theory of statistical intensity fluctuation correlation.

Following the above philosophy, we have measured the second-order correlation of incoherent radiations of A and B and observed a surprising nontrivial anticorrelation. Interestingly, the anticorrelation turns more significant after we subtract the contributions of possible self-correlations of the radiation A and the possible self-correlations of the radiation B from the joint measurement.

II. ANTICORRELATION FROM FIRST- AND SECOND-ORDER INCOHERENT THERMAL LIGHT

The anticorrelation experiment is schematically illustrated in Fig. 3. As we have mentioned in the Introduction, we bring the first- and second-order incoherent radiations A and B together by a 50%-50% beam splitter BS2. It is easy to see that if the two input fiber tips A and B are placed within the longitudinal coherence time and the transverse coherence area of the thermal field, i.e., $\Gamma^{(1)}_{AB}\neq 0$, this setup is equivalent to a Mach-Zehnder interferometer. D_1 and D_2 will each observe first-order interference as a function of the optical delay δ when scanning the fiber tip A along its longitudinal axis. Consequently, the joint-detection of D_1 and D_2 produces an interference that is factorizable into two first-order interferences.[3] However, in this experiment we decided

[3]It has been commonly accepted to consider a second-order interference trivial, if it is the product of two first-order interferences.

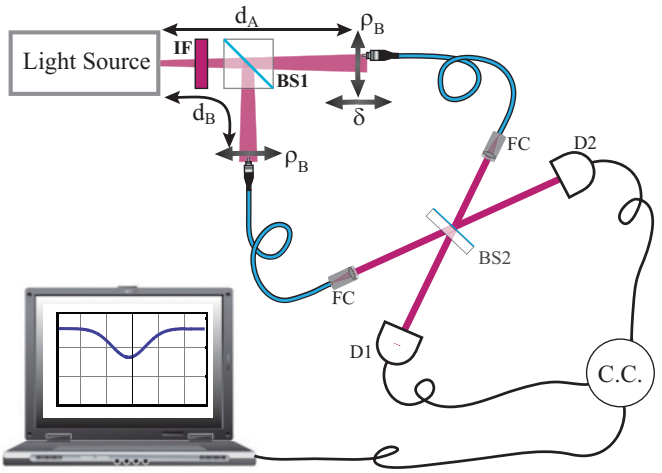

FIG. 3. (Color online) Schematic setup of the experiment. The pseudothermal light source consists of a $\lambda = 780$ nm pulsed laser radiation (∼150 fs) and a fast rotating diffusing ground glass. IF is an interference filter with 1 nm bandwidth. Pseudothermal light is split by a nonpolarizing beam-splitter cube BS1 and coupled into two fibers A and B. At the ends of the fibers, two fiber collimators (FCs) collimate two output beams into another nonpolarizing beam splitter BS2.

to move the fiber tip A outside the transverse coherence area to force $\Gamma^{(1)}_{AB} = 0$ and $\Gamma^{(2)}_{AB} = \langle E^*_A E_A E^*_B E_B \rangle = \text{constant}$. Under this condition, radiation A and B are first-order and second-order incoherent, there would be no first-order interference for any instantaneous "single-exposure" observation [12], and no intensity fluctuation correlation at all. The two radiations A and B are completely independent with random relative intensity fluctuations.

The measurement produced quite a surprise. An "unexpected" anticorrelation "dip" was observed in the joint-detection counting rate of D_1 and D_2 as functions of the optical delay δ while the single-detector counting rate of D_1 and D_2 both remained constants. The width of the dip is determined by the bandwidth of the spectral filters IF. Figure 4 reports two typical measured anticorrelation functions with different spectrum bandwidths of the chaotic-thermal field.

The experimental detail is described as follows:

(1) The source: The light source is a standard pseudothermal source that was developed in the 1960s and used widely in HBT correlation measurements [13]. The source consists of a $\lambda = 780$ nm laser radiation and a fast rotating diffusing ground glass. The laser is a CW mode-locked Ti:sapphire laser beam with ∼150 femtosecond pulses at a 78 MHz repetition rate. The linearly polarized laser beam is enlarged transversely onto the ground glass with a diameter of 4.5 mm. The enlarged laser radiation is scattered and diffused by the rotating ground glass to simulate a near-field, chaotic-thermal radiation source: a large number of independent point subsources with independent, stochastic, relative phases.

(2) The interferometer: A 50-50 nonpolarizing beam splitter (BS1) is used to split the chaotic-thermal light into transmitted and reflected radiations which are then coupled into two identical polarization-controlled single-mode fibers A and B respectively. The fiber tips are located ∼200 mm from the ground glass; i.e., $d_A = d_B \sim 200$ mm. At this distance, the angular size $\Delta\theta$ is ∼22.5 milliradians (1.29°) with respect to each input fiber tip, which satisfies the Fresnel near-field condition. The transverse coherence length of the radiation at the fiber tips is $l_c \sim 35\ \mu$m. A narrow-band spectral filter (IF) is employed. The transverse and longitudinal coordinates of the input fiber tips are both scannable by step motors. The output ends of the two fibers can be directly coupled into two single-photon avalanche detectors for near-field HBT correlation measurements or coupled into the two input ports of another 50-50 nonpolarizing beam splitter(BS2) for the anticorrelation measurement.

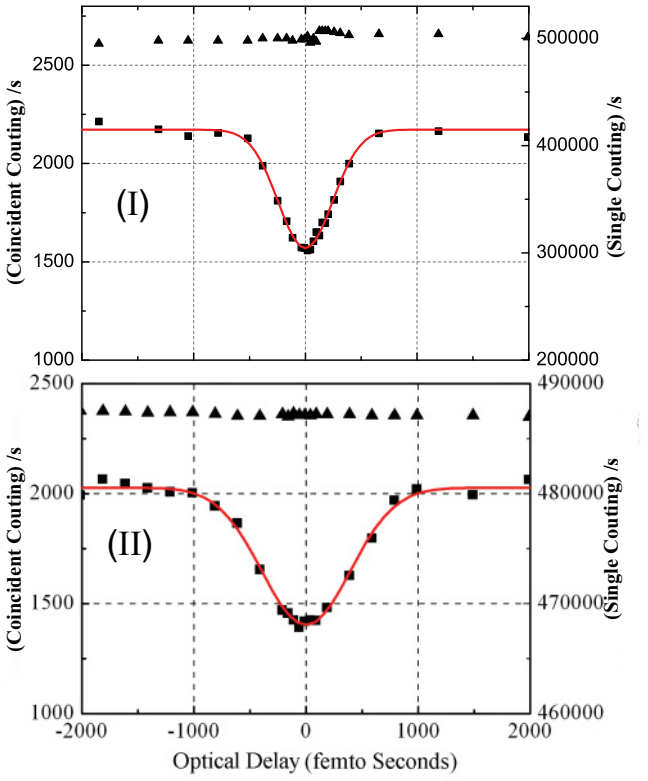

FIG. 4. (Color online) (Typical observed anticorrelation functions with different special bandwidth: $\tau_c \sim 345$ fs for (I), $\tau_c \sim 541$ fs for (II). The temporal width of the "dip" is determined by the bandwidth of the spectral filters (IF). The counting rates of D_1 and D_2 are both kept constant during the scanning of δ.

(3) The measurement: Two steps of measurements were made. The purpose of step one is to confirm that the light source produces chaotic-thermal field. We measured the HBT temporal and spatial correlation by scanning the input fiber tips longitudinally and transversely. In this measurement the output ends of the fibers are coupled into D_A and D_B directly as shown in Fig. 1. Chaotic-thermal radiation can easily be distinguished from coherent radiation by examining its second-order coherence function $G^{(2)}(\mathbf{r}_A, t_A; \mathbf{r}_B, t_B)$, which is characterized experimentally by the coincidence counting rate that counts the joint-photodetection events at space-time points $(\mathbf{r}_A, t_A)$ and $(\mathbf{r}_B, t_B)$.

In fact, any second-order effect would be trivial if it can be factorized into a product of two first-order effects.

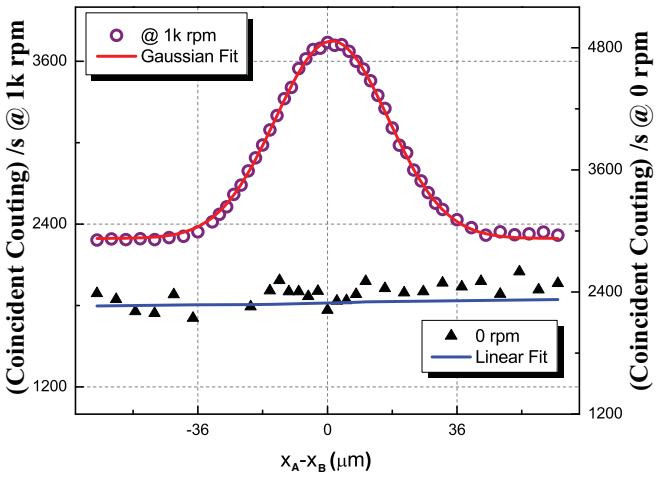

FIG. 5. (Color online) Measurement of $G^{(2)}(x_A - x_B)$ at no rotation (0 rpm) and at 1000 rpm (the linear velocity is around 0.8 m/s). Here, x_A and x_B are the x components of $\vec{\rho}_A$ and $\vec{\rho}_B$, and correspondingly the y components are kept $y_A = y_B$.

Figure 5 reports two measured second-order spatial correlations at zero and at 1000 revolutions per minute (rpm) of the rotating ground glass by scanning the fiber tips transversely. This measurement guarantees a typical HBT spatial correlation of chaotic-thermal light at rotation speeds greater than 1000 rpm of the ground glass, indicating the chaotic-thermal nature of the light source. In this measurement, we have also experimentally located the longitudinal and transverse coordinates of the fiber tips A and B for achieving the maximum coincidence counting rate, corresponding to the maximum second-order correlation.

The second-order temporal correlation peak is reported in Fig. 6. In this measurement, the joint-photodetection counting rate of D_A and D_B is measured as a function of $t_A - t_B$, where t_A and t_B are the registration times of D_A and D_B. The width of the temporal correlation peak is mainly determined by the response time of the photodetectors, which is around 1 ns, at least two orders greater than the width of the thermalized pulses. In fact, if the scanning range of $t_A - t_B$ is within a few

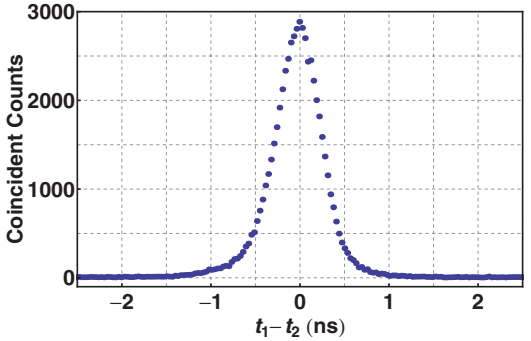

FIG. 6. (Color online) Measurement of $G^{(2)}(t_A - t_B)$ in an HBT type setup that is shown in Fig. 1 (by removing BS2 from Fig. 3), where t_A and t_B are the registration times of D_A and D_B, respectively. The correlation width is approximately 1 ns, which is mainly determined by the response time of the detectors, although the temporal width of the pulsed pseudothermal light is around 1 ps.

picoseconds at the top of the peak (equivalent to scanning δ in Fig. 3), we can only observe a trivial flat correlation.

In step two, we couple the 50-50 fiber beam splitter (BS2) into the setup as shown in Fig. 3. This measurement was done in two steps. We first measured the first-order interference at $\vec{\rho}_A = \vec{\rho}_B$ by scanning the input fiber tip A longitudinally in the neighborhood of $d_A \sim 200$ mm. It is no surprise to have first-order interference in the counting rates of D_1 and D_2. When choosing $\vec{\rho}_A = \vec{\rho}_B$, the two input fiber tips are coupled within the spatial coherence area of the radiation field; we have effectively built a Mach-Zehnder interferometer. We then move the input fiber tip A transversely from $\vec{\rho}_A = \vec{\rho}_B$ to $|\vec{\rho}_A - \vec{\rho}_B| \gg l_c$. (In most of the measurements, $|\vec{\rho}_A - \vec{\rho}_B|$ was chosen to be $|\vec{\rho}_A - \vec{\rho}_B| \geqslant 40 l_c$.) Then we scan the input fiber tip A again longitudinally in the neighborhood of $d_A \sim 200$ mm. The optical delay between the plane $z = d_A \sim 200$ mm and the scanning input fiber tip A is labeled as δ in Fig. 3. We have thus achieved the expected experimental condition of $\Gamma^{(1)}_{AB}(\mathbf{r}_A, t_A; \mathbf{r}_B, t_B) = 0$. It is no surprise that we lose any first-order interference in this experimental condition. However, it is indeed a surprise that an anticorrelation is observed in terms of the joint detection of D_1 and D_2 as a function of the optical delay δ that is reported in Fig. 4. In these measurements, $|\vec{\rho}_A - \vec{\rho}_B| \sim 40 l_c$.

Where does the anticorrelation dip come from? One suspicion is that the beam splitter may split the intensity A and the intensity B into two, respectively, and the observed correlation from the joint photodetection of D_1 and D_2 could be the intensity fluctuation correlation of the A field itself and the B field itself. In fact, the self-intensity correlation of the A field and B field are easy to be identified, respectively, by blocking the other beam. We have measured (1) the self-intensity correlation of the A field by blocking the radiation B, and (2) the self-intensity correlation of the B field by blocking the radiation A. These self-intensity correlation contributions can be easily subtracted from the correlation measurement of D_1 and D_2. If the correlation turns out to be a constant after the subtraction, the above suspicion is true. However, the measurement showed us, again, another surprise. The anticorrelation becomes more significant after the subtraction. Figure 7 reports the second-order correlation measurement of D_1 and D_2 after the subtraction of the self-intensity correlations of the A field and B field. The contrast of the anticorrelation becomes ~100%, which is very similar to the historical Hong-Ou-Mandel and Alley-Shih measurements (in the Alley-Shih experiment, a correlation "peak" is also observable) [14,15] on an entangled photon pair.

III. A SIMPLE QUANTUM MODEL OF TWO-PHOTON INTERFERENCE

In this section we give a simple quantum model to explain the experimental result as two-photon interference. In the experiment, the light source is a pseudothermal source, which has been studied experimentally and theoretically, and can be treated as a thermal source in general [13,16,17].[4] The

[4]A recent experimental and theoretical study of pulsed pseudothermal light will be submitted for publication soon.

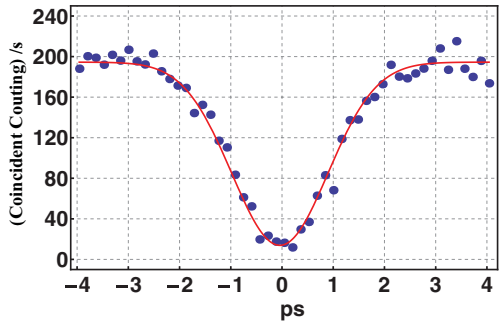

FIG. 7. (Color online) A typical measured temporal anticorrelation between D_1 and D_2 as function of the optical delay δ, after the subtraction of the self-intensity correlation of the A field and B field, which were measured by blocking the B field or A field, respectively. The visibility increased to $(92.9 \pm 3.7)\%$.

fast rotating ground glass contains a large number randomly distributed and shaped "scattering points" that scatter the laser beam into a large number of randomly distributed subfields in space-time with random phases. To simplify the discussion, we assume the light is weak enough to be at the single-photon level. It is reasonable to model fields A and B as two pointlike independent subradiations; each is produced by a large number of independent and randomly radiated wave packets:

$$\begin{aligned} \left|\psi_m^A\right\rangle &= \int d\omega\, h(\omega)\, e^{i\omega t_{0m}^A}\, \hat{a}^\dagger(\omega)\,|0\rangle, \\ \left|\psi_n^B\right\rangle &= \int d\omega\, h(\omega)\, e^{i\omega t_{0n}^B}\, \hat{b}^\dagger(\omega)\,|0\rangle, \end{aligned} \tag{6}$$

where A and B label the independent A field and B field, and m and n label the mth and the nth scattered wave packet. We have assumed an identical amplitude distribution $h(\omega)$ for all wave packets, which is consistent with the nature of the pseudothermal source, and randomly distributed t_{0m}^A and t_{0n}^B, which determine the phases of the wave packets at points A and B, respectively. From the source, each wave packet propagates to all possible directions. The subfields are superposed at the pointlike fiber tips.

The joint-photodetection counting rate is proportional to the second-order coherence function $G^{(2)}(\mathbf{r}_1,t_1;\mathbf{r}_2,t_2)$ that is calculated from

$$\begin{aligned} G_{12}^{(2)} &= \langle\langle \hat{E}_1^{(-)}\hat{E}_2^{(-)}\hat{E}_2^{(+)}\hat{E}_1^{(+)}\rangle_{\mathrm{QM}}\rangle_{\mathrm{Es}} \\ &= \left\langle \sum_{m<n} \left\langle\psi_m^A\right|\left\langle\psi_{m'}^A\right|\hat{E}_1^{(-)}\hat{E}_2^{(-)}\hat{E}_2^{(+)}\hat{E}_1^{(+)}\left|\psi_m^A\right\rangle\left|\psi_{m'}^A\right\rangle \right\rangle_{\mathrm{Es}} \\ &\quad + \left\langle \sum_{m<n} \left\langle\psi_n^B\right|\left\langle\psi_{n'}^B\right|\hat{E}_1^{(-)}\hat{E}_2^{(-)}\hat{E}_2^{(+)}\hat{E}_1^{(+)}\left|\psi_n^B\right\rangle\left|\psi_{n'}^B\right\rangle \right\rangle_{\mathrm{Es}} \\ &\quad + \left\langle \sum_{n,m} \left\langle\psi_m^A\right|\left\langle\psi_n^B\right|\hat{E}_1^{(-)}\hat{E}_2^{(-)}\hat{E}_2^{(+)}\hat{E}_1^{(+)}\left|\psi_m^A\right\rangle\left|\psi_n^B\right\rangle \right\rangle_{\mathrm{Es}} \\ &\equiv G_{AA}^{(2)} + G_{BB}^{(2)} + G_{AB}^{(2)}. \end{aligned} \tag{7}$$

Here we have applied the Glauber-Scully theorem in which we take the quantum expectation (denoted by $\langle\ldots\rangle_{QM}$) first and then take the statistical ensemble average (denoted by $\langle\ldots\rangle_{Es}$) [9,10]. Since the A and B fields are mutually incoherent, the second-order correlation can be separated into three distinguishable terms, $G_{AA}^{(2)}$, $G_{BB}^{(2)}$, and $G_{AB}^{(2)}$, which represent three kinds of joint-detection events: (1) both "clicks" on the detectors come from the A field; (2) both come the from B field; (3) one "click" comes from the A field, while another is from the B field. Explicitly,

$$\begin{aligned} G_{AA}^{(2)} &= \left\langle \sum_{m<n} \left|\langle 0|\hat{E}_2^{(+)}\hat{E}_1^{(+)}\left|\psi_m^A\right\rangle\left|\psi_n^A\right\rangle\right|^2 \right\rangle_{\mathrm{Es}} \\ G_{BB}^{(2)} &= \left\langle \sum_{m<n} \left|\langle 0|\hat{E}_2^{(+)}\hat{E}_1^{(+)}\left|\psi_m^B\right\rangle\left|\psi_n^B\right\rangle\right|^2 \right\rangle_{\mathrm{Es}} \\ G_{AB}^{(2)} &= \left\langle \sum_{n,m} \left|\langle 0|\hat{E}_2^{(+)}\hat{E}_1^{(+)}\left|\psi_m^A\right\rangle\left|\psi_n^B\right\rangle\right|^2 \right\rangle_{\mathrm{Es}} \\ &= \left\langle \sum_{n,m} \left|\Psi_{mn}^{AB}(z_1,t_1;z,t_2)\right|^2 \right\rangle_{\mathrm{Es}}, \end{aligned} \tag{8}$$

where we have assumed equal probability for the excitation of the mth and nth wave packets, and $\Psi_{mn}^{AB}(z_1,t_1;z_2,t_2)$ represents an effective wave function.

Following Eq. (8) and applying the wave packets of Eq. (6), it is not difficult to find that each $G_{AA}^{(2)}$ and $G_{BB}^{(2)}$ contribute to the joint-photodetection an HBT type correlation when D_1 and D_2 are placed with equal distances from the beam splitter BS2 to satisfy within $\tau_1 = \tau_2$. The quantum model gives the same result as that of Eq. (1). In this experiment, $G_{AA}^{(2)}$ and $G_{BB}^{(2)}$ both keep their normalized value of $g_{AA}^{(2)} = g_{BB}^{(2)} = 2$ during the scanning of the optical delay δ. We will not repeat the calculation for $G_{AA}^{(2)}$ and $G_{BB}^{(2)}$ as they are typical HBT correlations. Regarding $G_{AA}^{(2)}$ and $G_{BB}^{(2)}$, the most important observation in this experiment is that the contribution of $G_{AA}^{(2)}$ and $G_{BB}^{(2)}$, respectively, can be easily measured by blocking the B source or the A source, and can be legally subtracted from the direct measurement of $G_{AA}^{(2)} + G_{BB}^{(2)} + G_{AB}^{(2)}$.

Assuming the measurements of D_1 and D_2 are both in the far field, the field operators are approximated in the following form:

$$\begin{aligned} \hat{E}^{(+)}(z_1,t_1) &= \frac{1}{\sqrt{2}}[\hat{E}^{(+)}(\tau_{A1}) + \hat{E}^{(+)}(\tau_{B1})] \\ &= \frac{1}{\sqrt{2}}\int f(\omega)[\hat{a}_1(\omega)\, e^{i\omega\tau_{A1}} + \hat{b}_1(\omega)\, e^{i\omega\tau_{B1}}]d\omega, \\ \hat{E}^{(+)}(z_2,t_2) &= \frac{1}{\sqrt{2}}[\hat{E}^{(+)}(\tau_{A2}) - \hat{E}^{(+)}(\tau_{B2})] \\ &= \frac{1}{\sqrt{2}}\int f(\omega)[\hat{a}_2(\omega)\, e^{i\omega\tau_{A2}} - \hat{b}_2(\omega)\, e^{i\omega\tau_{B2}}]d\omega, \end{aligned} \tag{9}$$

where $\tau_{Aj} \equiv t_j - n(z_j - z_A)/c$, $\tau_{Bj} \equiv t_j - n(z_j - z_B)/c$, $j = 1,2$, is the optical delay from the detector D_j to the input planes A and B, respectively, and n is the index of refraction of the fiber. $f(\omega)$ specifies the spectral distribution of the field that is determined by the spectral function of the interference filter (IF). The "$-$" sign in $\hat{E}^{(+)}(z_2,t_2)$ is introduced by the beam splitter BS2. Then, the effective

wave function $\Psi_{mn}^{AB}(z_1,t_1;z_2,t_2)$ has two amplitudes that are superposed destructively:

$$\Psi_{mn}^{AB}(z_1,t_1;z_2,t_2) = \mathscr{A}_{mn}\left(\tau_{A1}^{R},\tau_{B2}^{R}\right) - \mathscr{A}_{nm}\left(\tau_{B1}^{T},\tau_{A2}^{T}\right). \quad (10)$$

Therefore,

$$G_{AB}^{(2)} = \left\langle \sum_{n,m} \left|\mathscr{A}_{mn}\left(\tau_{A1}^{R},\tau_{B2}^{R}\right)\right|^2 \right\rangle_{\mathrm{Es}} + \left\langle \sum_{n,m} \left|\mathscr{A}_{nm}\left(\tau_{B1}^{T},\tau_{A2}^{T}\right)\right|^2 \right\rangle_{\mathrm{Es}} - \left[\left\langle \sum_{n,m} \mathscr{A}_{mn}\left(\tau_{A1}^{R},\tau_{B2}^{R}\right)\mathscr{A}_{nm}^{*}\left(\tau_{B1}^{T},\tau_{A2}^{T}\right) + \mathrm{c.c.} \right\rangle_{\mathrm{Es}} \right]. \quad (11)$$

It is easy to see from Eqs. (10) and (11) that an anticorrelation function of $G_{AB}^{(2)}$ is expected, if $\mathscr{A}_{mn}(\tau_{A1},\tau_{B2})$ and $\mathscr{A}_{nm}(\tau_{B1},\tau_{A2})$ "overlap" completely (quantum mechanically indistinguishable) from one joint-photodetection event to another joint-photodetection event, for all m and n, in the ensemble average. Different from entangled states, a joint-photodetection event of thermal light is produced by two independent and randomly distributed photons that fall into the coincidence time window by chance only. Obtaining observable two-photon interference, we need (1) to achieve overlap of the two wave packets in a joint-photodetection event and (2) to achieve overlap of the two wave packets in all joint-photodetection events of an ensemble.[5]

The first critical issue we are facing is then how to overlap the two-photon amplitudes $\mathscr{A}(\tau_{A1},\tau_{B2})$ and $\mathscr{A}(\tau_{B1},\tau_{A2})$. Examining wave packets $\mathscr{A}_{mn}(\tau_{A1},\tau_{B2})$ and $\mathscr{A}_{nm}(\tau_{B1},\tau_{A2})$ by assuming a Gaussian spectrum of $f(\omega)$ with coherence time of t_c and central frequency at ω_0, it is straightforward to find

$$\mathscr{A}_{mn}(\tau_{A1},\tau_{B2}) = e^{-(\tau_{A1}-t_{0m}^{A})^2/t_c^2} e^{-(\tau_{B2}-t_{0n}^{B})^2/t_c^2} \times e^{-i\omega_0[(\tau_{A1}-t_{0m})+(\tau_{B2}-t_{0n})]}$$

$$\mathscr{A}_{nm}(\tau_{B1},\tau_{A2}) = e^{-(\tau_{B1}-t_{0n}^{B})^2/t_c^2} e^{-(\tau_{A2}-t_{0m}^{A})^2/t_c^2} \times e^{-i\omega_0[(\tau_{B1}-t_{0n})+(\tau_{A2}-t_{0m})]}.$$

To examine the overlapping-nonoverlapping of the two wave packets, we examine the envelopes of the two wave packets along the axis of t_1+t_2 and t_1-t_2:

$$\begin{aligned} & e^{-(\tau_{A1}-t_{0m}^{A})^2/t_c^2} e^{-(\tau_{B2}-t_{0n}^{B})^2/t_c^2} \\ &= e^{-\{[(t_1+t_2)-(t_{0m}^{A}+t_{0n}^{B})]-(z_1+z_2-z_A-z_B)/c\}^2/2t_c^2} \\ &\quad \times e^{-\{(t_1-t_2)-[(t_{0m}^{A}-t_{0n}^{B})-\delta]\}^2/2t_c^2}, \\ &\quad \times e^{-(\tau_{B1}-t_{0n}^{B})^2/t_c^2} e^{-(\tau_{A2}-t_{0m}^{A})^2/t_c^2} \\ &= e^{-\{[(t_1+t_2)-(t_{0n}^{B}+t_{0m}^{A})]-(z_1+z_2-z_A-z_B)/c\}^2/2t_c^2} \\ &\quad \times e^{-\{(t_1-t_2)-[(t_{0n}^{A}-t_{0m}^{B})-\delta]\}^2/2t_c^2}, \end{aligned} \quad (12)$$

where $\delta = (z_A - z_B)/c$ (note that $z_1 = z_2$ in the experiment). It is not too difficult to find that the two wave packets overlap completely along the axis of t_1+t_2; however, even if taking $\delta = 0$, the two wave packets can never overlap completely along the axis of $t_1 - t_2$, except when $t_{0m}^{A} = t_{0n}^{B}$. It is easy to achieve $\delta = 0$, while it is definitely nontrivial to achieve $t_{0m}^{A} = t_{0n}^{B}$ for thermal light. This situation is similar to what we have shown in Fig. 8. However, if we can make all the atomic transitions occur within a short time window to achieve $|t_{0m}^{A} - t_{0n}^{B}| < t_c$, $\mathscr{A}_{mn}(\mathbf{r}_A,t_A;\mathbf{r}_B,t_B)$ and $\mathscr{A}_{nm}(\mathbf{r}_A,t_A;\mathbf{r}_B,t_B)$ can partially overlap. Figure 8 illustrates a situation in which $|t_{0m}^{A} - t_{0n}^{B}| \ll t_c$ by applying a short pulse to excite the wave packets at points A and B. It is easy to see that shorter values of $|t_{0m}^{A} - t_{0n}^{B}|$ lead to a higher degree of overlapping between $\mathscr{A}_{mn}(\tau_{A1},\tau_{B2})$ and $\mathscr{A}_{nm}(\tau_{B1},\tau_{A2})$, and thus we may observe a higher degree of second-order coherence. In Dirac's language, we have achieved the condition for randomly paired photons to interfere with the pair itself.

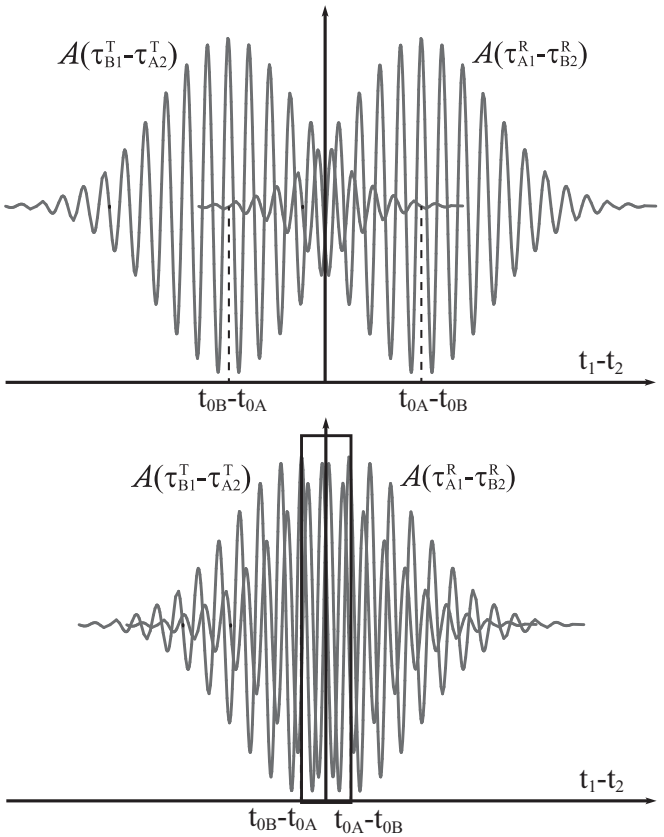

FIG. 8. Naturally, $\mathscr{A}_{mn}(\mathbf{r}_A,t_A;\mathbf{r}_B,t_B)$ and $\mathscr{A}_{nm}(\mathbf{r}_A,t_A;\mathbf{r}_B,t_B)$ can never be completely overlapped except when having $t_{0m}^{A} = t_{0n}^{B}$ by chance, which is almost zero. However, if we can force $|t_{0m}^{A} - t_{0n}^{B}| < t_c$ by applying a short pulse to excite the randomly paired mth and the nth atomic transition, we can make $\mathscr{A}_{mn}(\mathbf{r}_A,t_A;\mathbf{r}_B,t_B)$ and $\mathscr{A}_{nm}(\mathbf{r}_A,t_A;\mathbf{r}_B,t_B)$ partially overlap. The shorter $|t_{0m}^{A} - t_{0n}^{B}|$ we choose the more overlapping we may observe. The overlapping may achieve to ~100% if we can make $|t_{0m}^{A} - t_{0n}^{B}| \ll t_c$.

We now consider the second critical issue: the statistical ensemble average. In general, the inhomogeneous ensemble average of thermal fields would average out the two-photon interference when the $G^{(2)}$ measurement includes all possible randomly paired atomic transitions occurring at time from $-\infty$ to $+\infty$. What we can do is to force all the possible atomic transitions to occur within a restricted time interval. Assuming random temporal distributions of t_{0m}^{A} and t_{0n}^{B} in a limited time

[5]Entangled states achieve these two conditions in nature. For instance, (1) the signal-idler photon pair of SPDC is generated simultaneously; (2) the biphoton state is a pure state; i.e., all signal-idler pairs are in the same state yielding a homogenous ensemble.

window of $|t_{0m}^A - t_{0n}^B| < p$, the ensemble average of the cross term in Eq. (11) can be approximated as

$$\left\langle \sum_{m<n} \mathscr{A}_{mn}(\tau_{A1},\tau_{B2})\mathscr{A}_{nm}^*(\tau_{B1},\tau_{A2}) \right\rangle_{\mathrm{Es}}$$
$$\simeq \int_p dt_{0m}dt_{0n}\mathscr{A}_{mn}(\tau_{A1},\tau_{B2})\mathscr{A}_{nm}^*(\tau_{B1},\tau_{A2})$$
$$= \frac{1}{2}\int dt_{0+}dt_{0-}S_p(t_{0-})\mathscr{A}_{mn}(\tau_{A1},\tau_{B2})\mathscr{A}_{nm}^*(\tau_{B1},\tau_{A2})$$
$$= \mathscr{N}\frac{t_c}{2p}\left[\mathrm{erf}\left(\frac{p-2\delta}{2t_c}\right)+\mathrm{erf}\left(\frac{p+2\delta}{2t_c}\right)\right]e^{-t_-^2/t_c^2}, \quad (13)$$

where we introduce a step function $S_p(t_{0-})$, $S_p(t_{0-}) = 1/p$ when $|t_{0-}| < p/2$, otherwise $S_p(t_{0-}) = 0$. p represents a pulse width. In Eq. (13), $t_- \equiv t_1 - t_2$, $t_+ \equiv t_1 + t_2$, $t_{0-} \equiv t_{0m} - t_{0n}$, and $t_{0+} \equiv t_{0m} + t_{0n}$; erf stands for an error function; $\mathscr{N} \equiv \sqrt{\pi}\int dt_{0+}e^{-(t_+ - t_{0+} - \tau_+)/t_c^2}$, with $\tau_+ = [(z_1 + z_2) - (z_A + z_B)]/c$.

Similarly, the two-photon self-coherence functions are calculated in the following:

$$\left\langle \sum_{m<n} |\mathscr{A}_{mn}(\tau_{A1},\tau_{B2})|^2 \right\rangle_{\mathrm{Es}} \simeq \int dt_{0m}dt_{0n}|\mathscr{A}_{mn}(\tau_{A1},\tau_{B2})|^2$$
$$= \mathscr{N}\frac{t_c}{2p}\left[\mathrm{erf}\left(\frac{p-2\delta+2t_-}{2t_c}\right)+\mathrm{erf}\left(\frac{p+2\delta-2t_-}{2t_c}\right)\right]$$

$$\left\langle \sum_{m<n} |\mathscr{A}_{nn}(\tau_{B1},\tau_{A2})|^2 \right\rangle_{\mathrm{Es}} \simeq \int dt_{0m}dt_{0n}|\mathscr{A}_{nm}(\tau_{B1},\tau_{A2})|^2$$
$$= \mathscr{N}\frac{t_c}{2p}\left[\mathrm{erf}\left(\frac{p+2\delta+2t_-}{2t_c}\right)+\mathrm{erf}\left(\frac{p-2\delta-2t_-}{2t_c}\right)\right].$$

From the above analysis, it is clear that when taking $p \sim 0$, the coincident counting rate becomes

$$R_{AB} = \int dt_1dt_2S(t_1-t_2)G_{AB}^{(2)} \propto 2 - 2e^{-\delta^2/t_c^2}, \quad (14)$$

where $S(t_1 - t_2)$ is a step function that simulates the coincidence time window.

The coincident counting rates of $G_{AA}^{(2)}$ and $G_{BB}^{(2)}$ simply give $R_{AA} = R_{BB} = 2$. Therefore, the total coincident counting rate is $R \propto 3 - e^{-\delta^2/t_c^2}$.

Figure 9 illustrates the typical measured contributions of $G_{AA}^{(2)}$ and $G_{BB}^{(2)}$ as well as the total contribution of $G_{AA}^{(2)} + G_{BB}^{(2)} + G_{AB}^{(2)}$. It is interesting to find that after subtracting $G_{AA}^{(2)} + G_{BB}^{(2)}$ from $G_{AA}^{(2)} + G_{BB}^{(2)} + G_{AB}^{(2)}$, the net contribution of $G_{AB}^{(2)} + G_{BA}^{(2)}$ gives an anticorrelation dip with almost 100% visibility. Figure 7 reports another typical measured anticorrelation dip in which $G_{AA}^{(2)} + G_{BB}^{(2)}$ is subtracted during the scanning of the input fiber tip. The visibility is $(92.9 \pm 3.7)\%$.

The above thermalized wave packet model of two-photon interference has given a reasonable quantitative and qualitative explanation to the experimentally observed anticorrelation.

In the following, we give another simple model that is closer to a true thermal light source, such as the sunlight, which leads to the same result as that of the above model. This

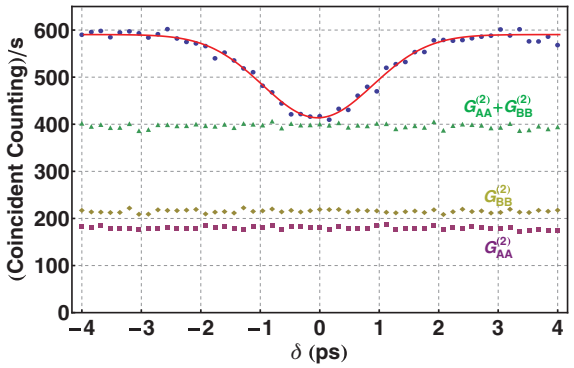

FIG. 9. (Color online) A typical measured $G_{AB}^{(2)} + G_{AA}^{(2)} + G_{BB}^{(2)}$, as well as $G_{AA}^{(2)}$ and $G_{BB}^{(2)}$ during the scanning of the optical delay δ. $G_{AA}^{(2)}$ and $G_{BB}^{(2)}$ were measured, respectively, by blocking the B source or the A source.

model assumes a collection of a large number of atoms that are ready for two-level atomic transitions at any time t. From the source, each atomic transition excites a subfield in the form of a symmetrical spherical wave propagating to all 4π directions. Although the chance to have a spontaneous emission is very small, there is indeed a small probability for an atom to create a photon whenever the atom decays from its higher energy level E_2 ($\Delta E_2 \neq 0$) down to its ground energy level of E_1. It is reasonable to assume the mth atomic transition excites a subfield in the following state:

$$|\psi_m\rangle = c_0|0\rangle + c_1\sum_s\int d\mathbf{k}h_m(\mathbf{k},s)\hat{a}_m^\dagger(\mathbf{k},s)|0\rangle$$
$$\simeq |0\rangle + \epsilon\sum_s\int d\mathbf{k}h_m(\mathbf{k},s)\hat{a}_m^\dagger(\mathbf{k},s)|0\rangle, \quad (15)$$

where $|c_0| \sim 1$ is the probability amplitude for no field excitation and $|c_1| = |\epsilon| \ll 1$ is the probability amplitude for the creation of a photon; $h_m(\mathbf{k},s) = \langle\psi_{\mathbf{k},s}|\psi_m\rangle$ is the complex probability amplitude for the radiation field to be in the Fock state of $|\psi_{\mathbf{k},s}\rangle = |1_{\mathbf{k},s}\rangle = \hat{a}^\dagger(\mathbf{k},s)|0\rangle$ with polarization s and $|\mathbf{k}| = \omega/c = (E_2 - E_1)/\hbar c$. The complex function $h_m(\mathbf{k},s)$ has a real and positive amplitude, which is mainly determined by the distribution of E_2 of the mth atom within ΔE_2, and a phase that is mainly determined by the transition time of the atom. In the following, we will focus on one polarization and drop the index s accordingly. The region of the integral on $|\mathbf{k}|$ is determined by ΔE_2 with $\Delta|\mathbf{k}| = (\Delta E_2 - E_1)/\hbar c$. The generalized state of the radiation field that is excited by the light source, which contains a large number atomic transitions, is formally written as

$$|\Psi\rangle = \prod_m\left\{|0\rangle + \epsilon c_m\int d\omega h_m(\omega)\hat{a}_m^\dagger(\omega)|0\rangle\right\} \simeq |0\rangle$$
$$+\epsilon\left[\sum_m c_m|\psi_m\rangle\right] + \epsilon^2\left[\sum_{m<n} c_mc_n|\psi_m\rangle|\psi_n\rangle\right] + \cdots, \quad (16)$$

where

$$|\psi_m\rangle \equiv \int d\omega\, h_m(\omega)\,\hat{a}_m^\dagger(\omega)\,|0\rangle$$

is the single-photon wave packet produced by the mth atomic transition at time t_{0m}, which determines the phase of the complex amplitude $h_m(\omega)$. Since $|\epsilon| \ll 1$, in Eq. (16) we listed the first-order and the second-order approximations on ϵ only.

The $G^{(2)}_{AB}$ can be calculated as

$$G^{(2)}_{AB} = \langle |\langle 0|\hat{E}^{(+)}_2 \hat{E}^{(+)}_1 |\Psi\rangle|^2 \rangle_{\rm Es}, \tag{17}$$

which is essentially the same as Eq. (8). Substituting the field operators and the states into Eq. (17), it is straightforward to obtain the same anticorrelation as that of Eq. (8).

Therefore, the above model of true thermal source as a collection of a large number of independent and randomly radiated atomic transitions will lead to the same result as that of thermalized wave packets.

IV. AN ANALYSIS BASED ON THE STANDARD GAUSSIAN STATISTICS OF THERMAL LIGHT

Quantum mechanics provides us a clear picture and reasonable model. Can a classical model lead us to the correct result? In this section we analyze the anticorrelation experiment by applying the standard Gaussian statistics of thermal light. In the standard Gaussian model, the second-order correlation function can be expressed in terms of the first-order correlation functions:

$$\langle E^*_1 E_1 E^*_2 E_2\rangle = \langle E^*_1 E_1\rangle\langle E^*_2 E_2\rangle + \langle E^*_1 E_2\rangle\langle E_1 E^*_2\rangle. \tag{18}$$

Complete information on the Gaussian field, such as chaotic-thermal, is provided by the first-order correlation functions [7,8].

The discussion will be divided into two steps: (1) a simplified discussion based on two sets of HBT measurements; (2) a more detailed calculation involving the propagation of radiation fields E_A and E_B.

Analysis 1. Examine the simplified schematic of the experimental setup of Fig. 10; since $\langle E^*_A E_B\rangle = 0$, there is no intensity fluctuation correlation between radiation fields A and B. Therefore, the first-order incoherent radiations A and B would not produce any interference (the detail is shown on the second step). So, we may treat the experimental setup as two sets of HBT interferometers with first-order and second-order

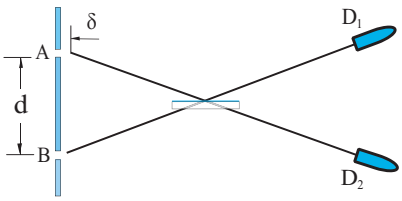

FIG. 10. (Color online) Simplified experimental setup. The radiation fields E_A and E_B are incoherent with $\langle E^*_A E_B\rangle = 0$.

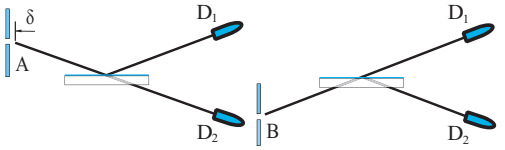

FIG. 11. (Color online) The anticorrelation setup combines two sets of independent HBT interferometers.

incoherent thermal sources A and B, respectively (Fig. 11). The HBT correlation is calculated from classical theory:

$$\begin{aligned}\Gamma^{(2)}_j(\mathbf{r}_1,t_1;\mathbf{r}_2,t_2) &= \langle I_{j1}(\mathbf{r}_1,t_1) I_{j2}(\mathbf{r}_2,t_2)\rangle = \langle E^*_{j1} E_{j1} E^*_{j2} E_{j2}\rangle \\ &= \langle E^*_{j1} E_{j1}\rangle\langle E^*_{j2} E_{j2}\rangle + \langle E^*_{j1} E_{j2}\rangle\langle E_{j1} E^*_{j2}\rangle \\ &= \Gamma^{(1)}_{j11}\Gamma^{(1)}_{j22} + \Gamma^{(1)}_{j12}\Gamma^{(1)}_{j21}, \end{aligned} \tag{19}$$

where $j = A,B$, E_{j1}, and E_{j2} label the radiation fields E_j at D_1 and D_2 to produce photodetection events of $(\mathbf{r}_1,t_1)$ and $(\mathbf{r}_2,t_2)$. Similar to Eq. (3), in Eq. (19) we have applied the statistical property of Gaussian light. It is easy to see that the first term in Eq. (19) is the product of two mean intensities of radiation j at $(\mathbf{r}_1,t_1)$ and $(\mathbf{r}_2,t_2)$. The second-term yields the nontrivial HBT correlation $|\Gamma^{(1)}_{j12}|^2$. If D_1 and D_2 are placed symmetrically with respect to slit A and slit B in which light takes equal optical paths, $z_{A1} - z_{A2} = 0$ and $z_{B1} - z_{B2} = 0$, to reach D_1 and D_2, the two independent HBT interferometers respectively thus give two independent sets of temporal HBT correlations:

$$\Gamma^{(2)}(\tau_1,\tau_2) \sim I^2_0\left\{1 + \mathrm{sinc}^2\left[\frac{\Delta\omega(\tau_1 - \tau_2)}{2}\right]\right\}. \tag{20}$$

It is clear that neither correlation is a function of the optical delay δ and there is no way to obtain an anticorrelation when scanning the optical delay δ. The above simple model failed to explain the experimental observations of Fig. 4.

Analysis 2. We consider a detailed calculation starting from

$$\begin{aligned}\Gamma^{(2)}(\mathbf{r}_1,t_1;\mathbf{r}_2,t_2) &= \langle I(\mathbf{r}_1,t_1) I(\mathbf{r}_2,t_2)\rangle = \langle (E^*_{A1} + E^*_{B1}) \\ &\quad \times (E_{A1} + E_{B1})(E^*_{A2} - E^*_{B2})(E_{A2} - E_{B2})\rangle, \end{aligned} \tag{21}$$

where E_{A1} and E_{B1} label the radiation fields at slit A and B in earlier times $t_1 - z_{A1}/c$ and $t_1 - z_{B1}/c$, respectively. We have sixteen expectations to evaluate:

$$\begin{aligned}&\langle I(\mathbf{r}_1,t_1) I(\mathbf{r}_2,t_2)\rangle \\ &= \langle E^*_{A1} E_{A1} E^*_{A2} E_{A2}\rangle + \langle E^*_{A1} E_{A1} E^*_{B2} E_{B2}\rangle \\ &- \langle E^*_{A1} E_{A1} E^*_{A2} E_{B2}\rangle - \langle E^*_{A1} E_{A1} E^*_{B2} E_{A2}\rangle \\ &+ \langle E^*_{B1} E_{B1} E^*_{A2} E_{A2}\rangle + \langle E^*_{B1} E_{B1} E^*_{B2} E_{B2}\rangle \\ &- \langle E^*_{B1} E_{B1} E^*_{A2} E_{B2}\rangle - \langle E^*_{B1} E_{B1} E^*_{B2} E_{A2}\rangle \\ &+ \langle E^*_{A1} E_{B1} E^*_{A2} E_{A2}\rangle + \langle E^*_{A1} E_{B1} E^*_{B2} E_{B2}\rangle \\ &- \langle E^*_{A1} E_{B1} E^*_{A2} E_{B2}\rangle - \langle E^*_{A1} E_{B1} E^*_{B2} E_{A2}\rangle \\ &+ \langle E^*_{B1} E_{A1} E^*_{A2} E_{A2}\rangle + \langle E^*_{B1} E_{A1} E^*_{B2} E_{B2}\rangle \\ &- \langle E^*_{B1} E_{A1} E^*_{A2} E_{B2}\rangle - \langle E^*_{B1} E_{A1} E^*_{B2} E_{A2}\rangle. \end{aligned} \tag{22}$$

Applying the property of Gaussian field and taking the result of $\langle E^*_A E_B\rangle = 0$, it is not too difficult to find that ten terms in

Eq. (22) take zero value, and leave six terms that may have nonzero contribution to $\langle I_1 I_2\rangle$:

$$\begin{aligned}\langle I(\mathbf{r}_1,t_1)I(\mathbf{r}_2,t_2)\rangle &= \langle E^*_{A1}E_{A1}E^*_{A2}E_{A2}\rangle + \langle E^*_{B1}E_{B1}E^*_{B2}E_{B2}\rangle \\ &+\langle E^*_{A1}E_{A1}E^*_{B2}E_{B2}\rangle + \langle E^*_{B1}E_{B1}E^*_{A2}E_{A2}\rangle \\ &-\langle E^*_{A1}E_{B1}E^*_{B2}E_{A2}\rangle - \langle E^*_{B1}E_{A1}E^*_{A2}E_{B2}\rangle. \end{aligned} \tag{23}$$

The first two terms in Eq. (23) correspond to the two sets of HBT correlations, similar to that in analysis 1:

$$\begin{aligned}\langle E^*_{A1}E_{A1}E^*_{A2}E_{A2}\rangle &= \langle E^*_{A1}E_{A1}\rangle\langle E^*_{A2}E_{A2}\rangle \\ &+ \langle E^*_{A1}E_{A2}\rangle\langle E^*_{A2}E_{A1}\rangle \\ &= \Gamma^{(1)}_{A11}\Gamma^{(1)}_{A22} + \Gamma^{(1)}_{A12}\Gamma^{(1)}_{A21}, \end{aligned} \tag{24}$$

$$\begin{aligned}\langle E^*_{B1}E_{B1}E^*_{B2}E_{B2}\rangle &= \langle E^*_{B1}E_{B1}\rangle\langle E^*_{B2}E_{B2}\rangle \\ &+ \langle E^*_{B1}E_{B2}\rangle\langle E^*_{B2}E_{B1}\rangle \\ &= \Gamma^{(1)}_{B11}\Gamma^{(1)}_{B22} + \Gamma^{(1)}_{B12}\Gamma^{(1)}_{B21}. \end{aligned} \tag{25}$$

It is clear that these two terms cannot produce the anticorrelation as a function of δ.

The next two terms in Eq. (23) are the products of mean intensities, which cannot produce the anticorrelation function of δ either:

$$\langle E^*_{A1}E_{A1}E^*_{B2}E_{B2}\rangle = \langle E^*_{A1}E_{A1}\rangle\langle E^*_{B2}E_{B2}\rangle = \Gamma^{(1)}_{A11}\Gamma^{(1)}_{B22}, \tag{26}$$

$$\langle E^*_{B1}E_{B1}E^*_{A2}E_{A2}\rangle = \langle E^*_{B1}E_{B1}\rangle\langle E^*_{A2}E_{A2}\rangle = \Gamma^{(1)}_{B11}\Gamma^{(1)}_{A22}. \tag{27}$$

The last two terms deal with the *self-correlation* of the A field and the B field, respectively. These two terms may contribute nonzero values to produce the nontrivial correlation; however, none of them is a function of the optical delay δ.

$$\langle E^*_{A1}E_{B1}E^*_{B2}E_{A2}\rangle = \langle E^*_{A1}E_{A2}\rangle\langle E^*_{B2}E_{B1}\rangle = \Gamma^{(1)}_{A12}\Gamma^{(1)}_{B21}, \tag{28}$$

$$\langle E^*_{B1}E_{A1}E^*_{A2}E_{B2}\rangle = \langle E^*_{B1}E_{B2}\rangle\langle E^*_{A2}E_{A1}\rangle = \Gamma^{(1)}_{B12}\Gamma^{(1)}_{A21}. \tag{29}$$

Physically, it is not difficult to see that $\Gamma^{(1)}_{A12}$ ($\Gamma^{(1)}_{A21}$) is associated with the A field only, and $\Gamma^{(1)}_{B21}$ ($\Gamma^{(1)}_{B12}$) is associated with the B field only. None of these first-order correlations give the information about the relative optical delay δ between the A field and the B field. Mathematically, it is not too difficult to find the following:

(1) The ensemble averages of $\Gamma^{(1)}_{A12}$ and $\Gamma^{(1)}_{B21}$,

$$\langle E^*_{A1}E_{A2}\rangle \sim \int d(\varphi_{0A} - \varphi'_{0A})E^*_{A1}E_{A2},$$

$$\langle E^*_{B1}E_{B2}\rangle \sim \int d(\varphi_{0B} - \varphi'_{0B})E^*_{B1}E_{B2},$$

are both independent of the optical delay δ, where φ_{0A} and φ_{0B} are the initial phases of the A field and B field. Consequently, the product of the two first-order correlation functions is also independent of the optical delay δ.

(2) The time averages of $\Gamma^{(1)}_{A12}$ and $\Gamma^{(1)}_{B21}$,

$$\langle E^*_{A1}E_{A2}\rangle \sim \int d(t_1 - t_2)S(t_1 - t_2)E^*_{A1}E_{A2},$$

$$\langle E^*_{B1}E_{B2}\rangle \sim \int d(t_1 - t_2)S(t_1 - t_2)E^*_{B1}E_{B2},$$

are both independent of the optical delay δ, where $S(t_1 - t_2)$ is a step function to simulate the function of coincidence time window. Consequently, the product of the two integrals is also independent of the optical delay δ. In this experiment the time window is a few nanoseconds; any possible time delay δ of picoseconds will be submerged in the relatively long time integrals. The results are all clearly independent of δ. Note that in this experiment $z_1 - z_A = z_2 - z_A$ and $z_1 - z_B = z_2 - z_B$ were chosen.

Therefore, the last two terms only contribute "noise" to the intensity-intensity correlation in terms of the optical delay δ. In classical theory, $\Gamma^{(1)}_{A12}$ and $\Gamma^{(1)}_{B21}$ (equivalently $\Gamma^{(1)}_{A21}$ and $\Gamma^{(1)}_{B12}$) may contribute to the joint-photodetection measurement of D_1 and D_2, respectively, whenever $t_1 - t_2$ falls into the coincidence time window.[6] However, in the experiment, the coincidence time window was set, to a few nanoseconds; the response time of the detectors is around a nanosecond, too, about 10^3 times greater than a picosecond, which is the range of δ. Even if there is a time delay between $\langle E^*_{A1}E_{A2}\rangle$ and $\langle E^*_{B1}E_{B2}\rangle$, the nanosecond measurement devices and their associated electronic circuits are definitely unable to distinguish any time delay in picosecond. To be able to distinguish a picosecond time delay by using a nanosecond measurement device, it is likely interference is involved. The physics is similar to that of the historical experiments, in which nanosecond measurement devices measured sub-picosecond time delay by using entangled photon pairs [14]. The interference involved in these experiments is well known as "two-photon interference" [17].

It is no surprise that the quantum theory of multiphoton interference and the classical theory of statistical intensity fluctuation correlation lead to different results. In terms of the ensemble average, the classical ensemble average is based on statistics of the first-order coherence functions $\Gamma^{(1)}$, such as

$$\langle E^*_{A1}E_{A2}\rangle_{\rm Es}\langle E^*_{B1}E_{B2}\rangle_{\rm Es}, \tag{30}$$

that are all second order of the field, while in the quantum model the ensemble average is based on the second-order correlation function

$$\begin{aligned}&\left\langle \sum_{n,m} \mathscr{A}_{mn}(\tau_{A1},\tau_{B2})\mathscr{A}^*_{nm}(\tau_{B1},\tau_{A2})\right\rangle_{\rm Es} \\ &= \left\langle \sum_{n,m} \langle\psi^{AB}_{mn}|\hat{E}^{(-)}(\tau_{B1})\hat{E}^{(-)}(\tau_{A2}) \right. \\ &\left. \times \hat{E}^{(+)}(\tau_{A1})\hat{E}^{(+)}(\tau_{B2})|\psi^{AB}_{mn}\rangle \right\rangle_{\rm Es}, \end{aligned} \tag{31}$$

which is fourth order in the field. Equations (30) and (31) are different in general, even if we may write Eq. (31) in a similar

[6] Different from quantum theory of light, classical theory does not prevent any weak light to contribute to an intensity-intensity correlation measurement. There is no lower energy limit for the measurement of intensity.

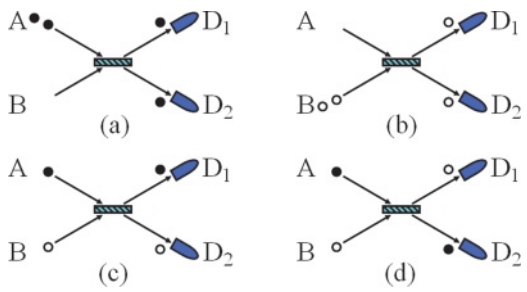

FIG. 12. (Color online) There are four alternative ways for a measured pair of independent photons to trigger a joint-detection event of D_1 and D_2.

form to the Gaussian model,

$$\left\langle \sum_{n,m} \mathscr{A}_{mn}\left(\tau_{A1}^{R},\tau_{B2}^{R}\right)\mathscr{A}_{nm}^{*}\left(\tau_{B1}^{T},\tau_{A2}^{T}\right)\right\rangle_{\mathrm{Es}}$$
$$= \left\langle \sum_{n,m} \left\langle \psi_n^B\middle|\hat{E}^{(-)}(\tau_{B1})\hat{E}^{(+)}(\tau_{B2})\middle|\psi_n^B\right\rangle \right.$$
$$\left. \times \left\langle \psi_m^A\middle|\hat{E}^{(-)}(\tau_{A2})\hat{E}^{(+)}(\tau_{A1})\middle|\psi_m^A\right\rangle \right\rangle_{\mathrm{Es}}. \qquad (32)$$

The ensemble average of a product of two functions is in general different from the product of the two ensemble averages. In a spectral measurement, such as the historical HBT observation of distant stars, the two cases lead to the same result; however, it is never true in general, especially in this experiment, that the results are very different.

V. SUMMARY

Based on the theory of Gaussian statistics of intensity fluctuations, we may never be able to understand the experimental observation of anticorrelation. For first-order and second-order incoherent radiations with $\Gamma^{(1)}(\mathbf{r}_A,t_A;\mathbf{r}_B,t_B)=0$ and $\Gamma^{(2)}(\mathbf{r}_A,t_A;\mathbf{r}_B,t_B)=$ constant, there should be no intensity fluctuation correlation between the A field and B field. The two intensity fluctuations are completely independent. How could the A field and B field produce an anticorrelation

$$G_{AB}^{(2)}(\mathbf{r}_1,t_1;\mathbf{r}_2,t_2)\propto 1-e^{-\delta^2/t_c^2}$$

in a later time after passing through a simple optical beam splitter? As we know, there is no nonlinear interaction between the two fields at such a simple beam splitter. Each field propagates freely according to the linear Maxwell wave equation, except for a phase delay.

In the view of quantum mechanics, the observed anticorrelation is the result of two-photon interference. Analogous to Dirac's statement that a photon interferes with itself, this interference is a jointly measured pair of independent photons interfering with the pair itself. Figure 12 schematically illustrates four alternatives for two independent photons to trigger a joint-detection event of D_1 and D_2. In panels (a) and (b) the measured pair comes from the same fiber tip, A or B. In panels (c) and (d) the measured pair comes from different fiber tips, one from A and the other from B. It is the superposition between amplitudes in panels (c) and (d) that produces the anticorrelation. We should note that we introduced a short pulse to make the two probability amplitudes almost completely overlap in order to observe a maximum anticorrelation.

In conclusion, we have observed the nonclassical anticorrelation of chaotic-thermal light under the experimental condition of $\Gamma_{AB}^{(1)}(\mathbf{r}_A,t_A;\mathbf{r}_B,t_B)=0$ and $\Gamma_{AB}^{(2)}(\mathbf{r}_A,t_A;\mathbf{r}_B,t_B)=$ constant. This observation is different from all historical measurements of the "dip," either observed from entangled two-photon sources or from synchronized coherent sources: (1) It is observed from chaotic-thermal light; (2) it is observed from first-order and second-order incoherent chaotic-thermal light. The classical statistical correlation theory seems unable to explain this experimental result. In the view of quantum mechanics, either the anticorrelation "dip" or the correlation "peak" of thermal light is a straightforward two-photon interference phenomenon, involving the constructive or destructive superposition of two-photon amplitudes.

ACKNOWLEDGMENTS

The authors wish to thank T. B. Pittman, M. H. Rubin, J. P. Simon, Y. Zhou, G. Scarcelli, and V. Tamma for helpful discussions. This research was partially supported by AFOSR and the ARO-MURI program. Z.X. acknowledges his partial support from the China Scholarship Council.

[1] R. Hanbury Brown and R. Q. Twiss, Nature (London) **177**, 27 (1956); R. Hanbury Brown, *Intensity Interferometer* (Taylor & Francis, London, 1974).

[2] R. Hanbury Brown and R. Q. Twiss, Nature (London) **178**, 1046 (1956).

[3] A. Valencia, G. Scarcelli, M. D'Angelo, and Y. Shih, Phys. Rev. Lett. **94**, 063601 (2005).

[4] A. Einstein, B. Podolsky, and N. Rosen, Phys. Rev. **47**, 777 (1935).

[5] G. Scarcelli, V. Berardi, and Y. H. Shih, Phys. Rev. Lett. **96**, 063602 (2006); R. Meyers, K. S. Deacon, and Y. H. Shih, Phys. Rev. A **77**, 041801(R) (2008).

[6] R. Hanbury Brown and R. Q. Twiss, Proc. R. Soc. London A **242**, 300 (1957).

[7] Joseph W. Goodman, *Statistical Optics*, 1st ed. (Wiley Interscience, 1985).

[8] D. N. Klyshko, *Photons and Nonlinear Optics* (Gorden and Breach Science, 1988).

[9] R. J. Glauber, Phys. Rev. **10**, 84 (1963); **130**, 2529 (1963). In Eq. (5), we use $G^{(2)}$ to distinguish quantum correlation from the classical statistical intensity correlation of $\Gamma^{(2)}$.

[10] M. O. Scully and M. S. Zubairy, *Quantum Optics*, 1st ed. (Cambridge University Press, Cambridge, 1997).

[11] The use of first-order and second-order incoherent thermal fields, $\Gamma_{AB}^{(1)}=0$, $\Gamma_{AB}^{(2)}=$ constant, makes this experiment different from all other demonstrations of coincidence "dip," such as that of Z. Y. Ou, E. C. Gage, B. E. Magill, and L. Mandel, J. Opt. Soc. Am. B. **6**, 100 (1989). In the experiment of Ou *et al.*, a

beam splitter splits the input light into two first-order coherent beams. The two beams are superposed at another beam splitter for the observation of first-order interference and second-order correlation. Although the use of a phase modulator in one arm disturbing the interferometer to change the phase of the interference pattern from time to time results in a time averaged constant output, the two superposed fields are still intrinsically first-order and second-order coherent. In our experiment, the A and B fields are first-order and second-order incoherent.

[12] Mandel *et al*. showed that radiations from two independent sources can produce first-order interference for an single-shot exposure, if the "exposure" time is shorter than the coherence time of the fields. See G. Magyar and L. Mandel, Nature (London) **198**, 255 (1963); L. Mandel, Phys. Rev. A **28**, 929 (1983). In a time integrated multiexposure measurement, the first-order interference pattern may not be observable due to the phase variation from one exposure to another exposure. However, the joint detection of two individual photodetectors may still produce observable second-order correlation or anticorrelation. In our experiment, $\Gamma^{(1)}_{AB}$ is chosen to be zero. The classical interpretation of time averaged effect of classical mutual coherence or partial mutual coherence does not apply.

[13] W. Martienssen and E. Spiller, Am. J. Phys. **32**, 919 (1964).

[14] C. K. Hong, Z. Y. Ou, and L. Mandel, Phys. Rev. Lett. **59**, 2044 (1987).

[15] C. O. Alley and Y. H. Shih, in *Proceedings of the Second International Symposium, Foundations of Quantum Mechanics in the Light of New Technology*, edited by M. Namiki *et al*. (Physical Society of Japan, Tokyo, 1987), p. 36; Y. H. Shih and C. O. Alley, Phys. Rev. Lett. **61**, 2921 (1988). In the Alley-Shih two-photon interferometer, both the anticorrelation "dip" and correlation "peak" are observable by selecting different Bell states (polarization correlation) of the entangled photon pair.

[16] J. Ohtsubo, Opt. Commun. **34**, 147 (1980); T. Asakura and N. Takai, Appl. Phys. **25**, 179 (1981); J. H. Churnside and H. T. Yura, Appl. Opt. **20**, 3539 (1981).

[17] Y. H. Shih, *An Introduction to Quantum Optics: Photon and Biphoton Physics*, 1st ed. (Taylor & Francis, 2011).